ACS APPLIED MATERIALS & INTERFACES

Research Article

www.acsami.org

Triplet–Triplet Annihilation Upconversion in CdS-Decorated SiO_2 Nanocapsules for Sub-Bandgap Photocatalysis

Oh Seok Kwon,[†] Jae-Hyuk Kim,[†,‡] Jin Ku Cho,[§] and Jae-Hong Kim*,[†]

[†]Department of Chemical and Environmental, Engineering School of Engineering and Applied Science, Yale University, New Haven, Connecticut 06511, United States

[‡]School of Civil and Environmental Engineering, Pusan National University, Busan 609-735, Republic Korea

[§]Green Process and Materials R&D Group, Korea Institute of Industrial Technology (KITECH), 89 Yangdaegiro-gil, Ipjang-myeon, Cheonan, 331-825 Chungnam Korea

Supporting Information

ABSTRACT: This study reports the first successful nanoscale encapsulation of triplet–triplet annihilation upconversion (TTA-UC) medium within a rigid silica shell using a self-assembly microemulsion process. These newly synthesized nanocapsules present a few critical advances that could be instrumental for a wide range of aqueous-based photonics applications, including photocatalysis, artificial photosynthesis, and bioimaging. The nanocapsules form a homogeneous suspension that can produce intense, diffuse UC emission in water without deoxygenation, closely resembling conventional TTA-UC processes that have been performed in deoxygenated organic solvents. The silica shell provides sites for further surface modification, which allows, when combined with its nanoscale dimension and structural rigidity, this TTA-UC system to acquire various useful functionalities. A benchmark TTA-UC pair, palladium(II) tetraphenyltetrabenzoporphyrin as a sensitizer and perylene as an acceptor, was used to demonstrate efficient red-to-blue (635 nm, 1.95 eV → 470 nm, 2.6 eV) upconversion in the oxygen-rich aqueous phase. The nanocapsule surface was further functionalized with cadmium sulfide nanoparticles (E_g = 2.4 eV) to demonstrate sub-bandgap sensitization and subsequent aqueous-phase catalytic oxidation.

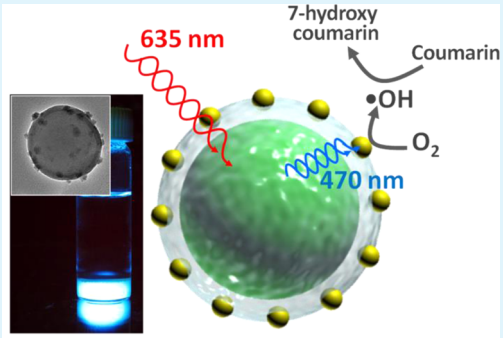

Aqueous-stable nano-scale encapsulation of TTA-UC

KEYWORDS: *triplet–triplet annihilation, upconversion, inorganic nanocapsules, photocatalysis, chromophores*

INTRODUCTION

Amplifying the frequency of noncoherent, low-energy photons through upconversion (UC) presents a unique strategy for enhancing the efficiency of solar-based technologies, including photovoltaics,[1−5] photosynthesis,[6−8] and photocatalysis,[9−13] as well as for exploring unconventional optical and imaging applications.[14−19] Among different approaches to achieve anti-Stokes shifting, UC based on the triplet–triplet annihilation (TTA) mechanism has been considered the most promising due to its unmatched quantum yield (3–40%) at low excitation intensities (1–10 mW/cm^2),[20] significantly higher than that of benchmark UC processes that utilize lanthanide-doped inorganic crystals.[21] TTA-UC is achieved by synchronous energy transfer processes between two organic chromophores (Supporting Information Figure S1); the first chromophore (sensitizer) absorbs low-energy photons and transfers this excitation energy to the second chromophore (acceptor) via intermolecular triplet–triplet energy transfer (TTET).[20] A pair of acceptors in the resulting long-lived triplet excited state undergoes another bimolecular energy transfer via TTA to produce an acceptor in the singlet excited state, which then fluoresces a photon with energy higher than that of the incident photons.[20]

Efficient TTA-UC occurs, however, only under severely restricted conditions. First, chromophores developed for TTA-UC to date are all organic or organometallic and thus soluble only in nonpolar media.[21] Second, since high chromophore mobility is necessary to facilitate the TTET and TTA energy transfer processes, most solid materials are not optimal host media for TTA-UC.[22] Third, TTA-UC host media should be devoid of oxygen, which quenches the sensitizer triplet excited state through the formation of singlet oxygen and thereby prevents TTET.[23,24] These restrictions are detrimental to the realization of TTA-UC in the oxygen-rich aqueous environment, which is highly desirable for many of the aforementioned applications. In particular, aqueous-phase UC could greatly enhance semiconductor photocatalysis for artificial photosynthesis and environmental remediation.[25,26] Semiconductors are sensitized only when the energy of incident photons exceeds

Received: September 11, 2014
Accepted: December 18, 2014
Published: December 18, 2014

DOI: 10.1021/am506233h
ACS Appl. Mater. Interfaces 2015, 7, 318–325

Scheme 1. Schematic Illustration of the Simple Two-Step SNC Fabrication Process Based on an Emulsion Self-Assembly

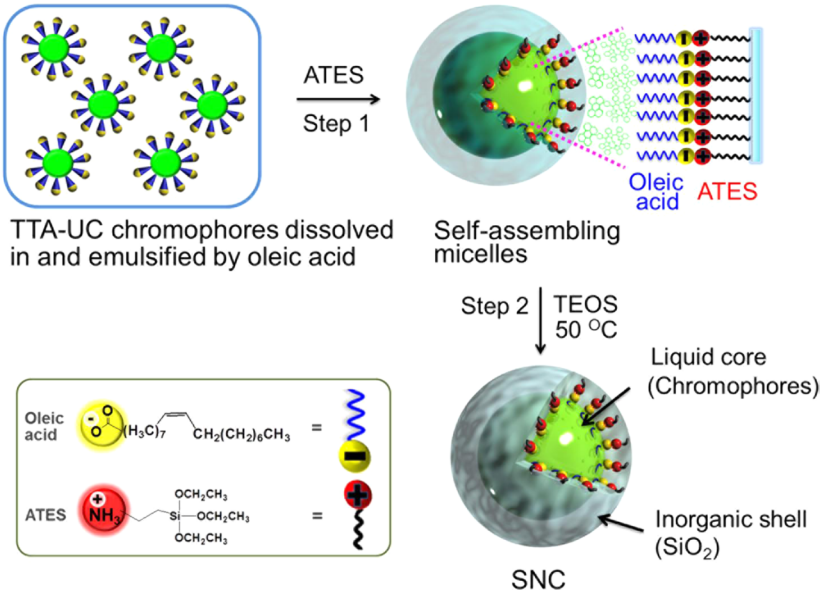

the bandgap energy,[27] so a large portion of the solar spectrum is typically not utilized. TTA-UC can improve the sensitization efficiency by amplifying the frequency of sub-bandgap photons that would otherwise be wasted.[21]

Many recent studies, therefore, have attempted to achieve efficient UC in the aqueous phase. Embedding TTA-UC chromophores in rubbery polymer particles[28,29] and porous silica particles[30] has proven relatively ineffective due to gradual oxygen penetration and obstruction of chromophore diffusion.[22] A more promising approach for efficient TTA-UC is the encapsulation of the chromophore-containing organic medium in a core−shell structure. The organic medium is often supplemented with molecules such as unsaturated hydrocarbons that quench singlet oxygen.[21] Alternatively, media such as soybean oil that quench singlet oxygen have been employed.[22] An ideal shell material for encapsulation of these media should be structurally rigid and enable further functionalization for specific applications. Micelle[31,32] and dendrimer[33,34] structures have been explored but are far from ideal. Shells that consist of biomaterials such as bovine serum albumin[22] and liposomes[35] have also been fabricated but suffer from structural instability, vulnerability to environmental shocks like pH and temperature variation, and difficulty of further surface loading (e.g., semiconductors). Crystalline polymer shells have been employed in our recent work[21] for the fabrication of stable aqueous- and dry-phase microcapsules. Unfortunately, the synthesis procedure based on a microfluidic device is complicated and does not allow for nanoscale encapsulation.

We herein present a new TTA-UC encapsulation architecture, herein termed silica nanocapsules (SNCs), which enables efficient UC in the oxygen-rich aqueous phase. This new TTA-UC system presents a number of departures from and advances over past designs. First, encapsulation of the chromophores dissolved in a continuous liquid phase allows for maximized chromophore diffusion due to the fluidic nature of the solvent. Second, use of silica for the nanocapsule shell provides structural robustness. Third, the combination of the nanocapsules' nanoscale dimension and the hydrophilicity of the silica surface enables near-homogeneous dispersion in water. Their increased surface area compared to their microscale counterparts is particularly advantageous for surface-area-dependent applications. Fourth, the silica surface provides sites for facile surface functionalization and anchoring of auxiliary materials such as photocatalysts, as demonstrated below. Finally, the fabrication is based on a simple and scalable self-assembling emulsion process.

EXPERIMENTAL METHODS

Fabrication of SNCs. Stock solutions of palladium(II) tetraphenyltetrabenzoporphyrin (PdTPBP, 20 mM; Frontier Scientific) and perylene (20 mM; Gelest Inc.) in tetrahydrofuran (THF, >99.9%; Aldrich) were prepared and kept in the dark prior to use. The stock solutions (125 μL PdTPBP solution and 300 μL perylene solution) were mixed with 5 mL oleic acid (OA, 90%; Aldrich) and stored overnight (12 h) in an oven at 70 °C to remove the THF. An aliquot (300 μL) of this mixture was emulsified in distilled water (28.8 mL) under sonication (Bransonic 2800, 40 kHz) for 5 min followed by vigorous stirring (over 1000 rpm) for 1 h; 1 mmol of (3-aminopropyl)triethoxysilane (ATES, 98%; Aldrich) was added dropwise (0.2 mL/min) to the emulsified mixture to obtain a micelle suspension. Tetraethyl orthosilicate (TEOS, 98%; Aldrich) was subsequently added at two different ATES/TEOS molar ratios (1:6 and 1:9) to yield SNCs with different shell thickness (see Results). The mixture was left at room temperature for ca. 1−2 h, gently mixed (150 rpm) for 25−30 h at 55 °C, and washed with distilled water and ethanol prior to further characterization.

Photoluminescence Measurement. The static absorption and Stokes emission spectra of the chromophores dissolved in oleic acid were analyzed on a UV−visible spectrophotometer (8453, Agilent) and spectrofluorophotometer (RF-5301, Shimadzu), respectively. Stokes and anti-Stokes emission spectra of the aqueous SNC suspension were obtained using a commercial diode laser (635 nm) as an excitation source. A cuvette containing the SNC suspension was irradiated by a laser beam incident at an angle of approximately 40° and the emission was collected through a series of focusing lenses and an optical chopper (120 Hz) before reaching a monochromator (Oriel Cornerstone, Newport Corp.). Incident laser power was adjusted using a series of neutral density filters and was measured using a Nova II power meter/photodiode detector head (Ophir). The signal was detected by an Oriel photomultiplier tube and processed by an Oriel Merlin radiometry detection system (Newport Corp.).

DOI: 10.1021/am506233h
ACS Appl. Mater. Interfaces 2015, 7, 318−325

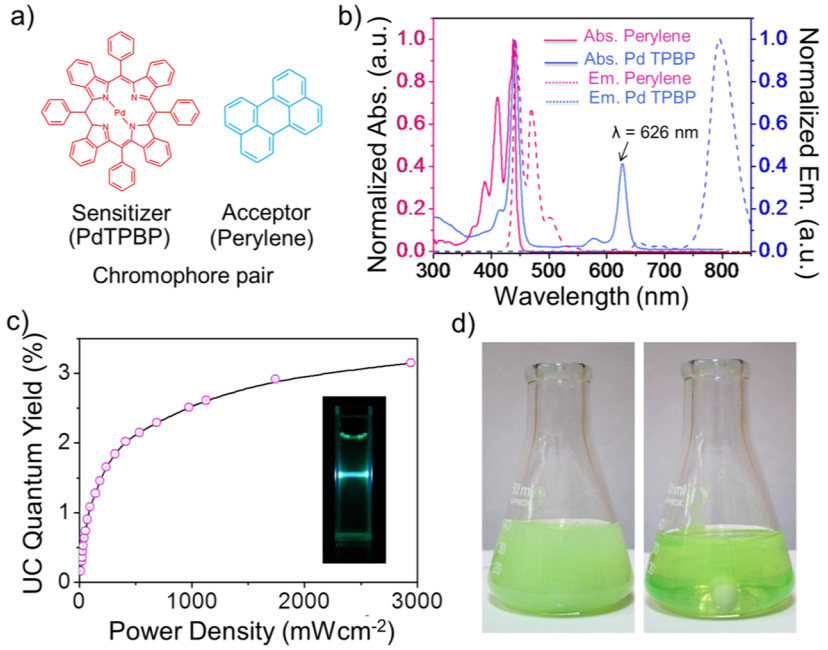

Figure 1. (a) Chemical structures of the sensitizer (PdTPBP) and acceptor (perylene) chromophore pair. (b) Normalized absorption (solid lines) and photoluminescence (dashed line) spectra of PdTPBP (cyan) and perylene (magenta). (c) UC quantum yield of PdTPBP/perylene system in OA as a function of laser power density (14−2950 mW/cm^2): [PdTPBP] = 36 μM and [perylene] = 485 μM. The inset shows a photograph of PdTPBP/perylene solution in OA upon red laser irradiation, demonstrating red-to-blue UC. (d) Photographs before and after the introduction of ATES into the OA emulsified mixture (right: the magnetic bar is clearly shown through the transparent mixture).

Fabrication of SNCs with Stearic Acid Core. The chromophore stock solutions as prepared above (125 μL PdTPBP solution and 300 μL perylene solution) were mixed with 4 mL THF containing 5 g stearic acid. The steps used above to fabricate OA-core SNCs were followed with this stearic acid mixture in place of the OA mixture to fabricate SNCs with a stearic acid core. Another set of SNCs with chromophores embedded inside the silica shell was also prepared. An aliquot (300 μL) of the stearic acid/THF solution prepared above was emulsified in distilled water (28.8 mL) under 5 min sonication and 1 h vigorous stirring. ATES (1 mmol) was first added dropwise (0.2 mL/min) to form a micelle suspension. The mixture of chromophore stock solutions (125 μL PdTPBP and 300 μL perylene solution) and TEOS (1.75 mL) was subsequently added dropwise to the suspension. The resulting mixture was left at room temperature for ca. 1−2 h. The mixture was then stored at 55 °C under gentle stirring for 25−30 h, after which it was washed with distilled water and ethanol.

CdS Nanoparticle Loading. The surface of the SNCs was first functionalized with amino groups using 0.69 mL (3-aminopropyl)-trimethoxysilane (APMS; Aldrich) under gentle mixing (150 rpm) at 55 °C for 25−30 h. After washing with distilled water, the SNC suspension was mixed with 20 mL cadmium chloride ($CdCl_2$; Aldrich) solution (0.1 M) for 4 h. Residue was removed by washing with distilled water. The suspension was further treated with 20 mL thioacetamide (CH_3CSNH_2; Aldrich) solution (0.1 M) under gentle mixing at 28.9 °C for 24 h. The final product was washed with distilled water.

Hydroxyl Radical Generation. A solution of coumarin in deionized water (Milli-Q, Millipore) (250 mg/L, 2 mL) was added to a suspension of CdS NP-decorated SNCs (2 mL, ∼ 50 v/v%). The sample suspension was irradiated with a red laser (635 nm) under gentle mixing (150 rpm) with a magnetic stirrer. Sample aliquots were withdrawn at 5, 10, 20, and 30 min after the start of irradiation and filtered using a 0.45 μm PTFE syringe filter to remove CdS NP-decorated SNCs. The fluorescence emission profile of 7-hydroxycoumarin was measured under excitation at 332 nm using a spectrofluorometer (Shimadzu RF-5301).

RESULTS AND DISCUSSION

Scheme 1 illustrates the newly established two-step procedure for SNC fabrication. The first step is the emulsification of chromophore/oleic acid (OA) solution in distilled water under sonication followed by vigorous stirring. OA was chosen based on both its ability to dissolve TTA-UC chromophores and on the compatibility of its anionic terminal groups with self-assembly using cationic surfactants.[36] More importantly, its unsaturated double bonds also quench singlet oxygen through the ene reaction (discussed further below). PdTPBP and perylene (Figure 1a) were selected as the sensitizer and acceptor, respectively, to fulfill the energy requirement for TTA-UC—that is, $E(^3\text{PdTPBP}^*) = 1.57$ eV[5] > $E(^3\text{perylene}^*) = 1.53$ eV.[37] PdTPBP dissolved in oleic acid has an intense Soret absorption band at 360−480 nm and Q-band at around 626 nm (Figure 1b). Upon irradiation with a 635 nm red laser, PdTPBP in oleic acid phosphoresces at approximately 800 nm even without deoxygenation (i.e., due to consumption of singlet oxygen by oleic acid). Perylene emits blue fluorescence at approximately 440 nm. When combined, this chromophore pair achieves red-to-blue upconversion, with increasing quantum yield (QY) at higher power density reaching ca. 3.1% at ca. 2950 mW/cm^2 (Figure 1c and Supporting Information (SI)), similar to previous reports.[21,22,37] The QY of PdTPBP/perylene has been reported to range from 0.5% in liposomes[35] to 1.2% in toluene,[35] and that of a similar chromophore pair (PtTPBP-(platinum(II) tetraphenyltetrabenzoporphyrin)/perylene) in mineral oil was reported to be 5.3%,[37] while direct comparison is not possible since the QY depends on various conditions including chromophore concentrations, solvent type, and incident light intensity. The OA solution containing PdTPBP and perylene appeared transparent, and a clear laser pathway with upconverted blue color was visible upon red laser beam irradiation (Figure 1c, inset). In contrast, the aqueous emulsion

DOI: 10.1021/am506233h
ACS Appl. Mater. Interfaces 2015, 7, 318−325

of OA-dissolved chromophores first appeared turbid due to the formation of micelles of a wide range of sizes (Figure 1d, left). When ATES was added, an ATES/OA micelle suspension formed via spontaneous self-assembly (Step 1 in Scheme 1). The suspension became transparent once more (Figure 1d, right), indicating the formation of nanoscale micellar templates. Addition of TEOS then initiated the growth of the SiO_2 network on the micelle surface (Step 2 in Scheme 1).

Field-emission scanning electron microscopy (FE-SEM; JSM-6700F) and high-resolution transmission electron microscopy (HR-TEM; JEM-3010(JEOL)) images of SNC samples (Figure 2a and b) suggest that the synthesized nanocapsules are

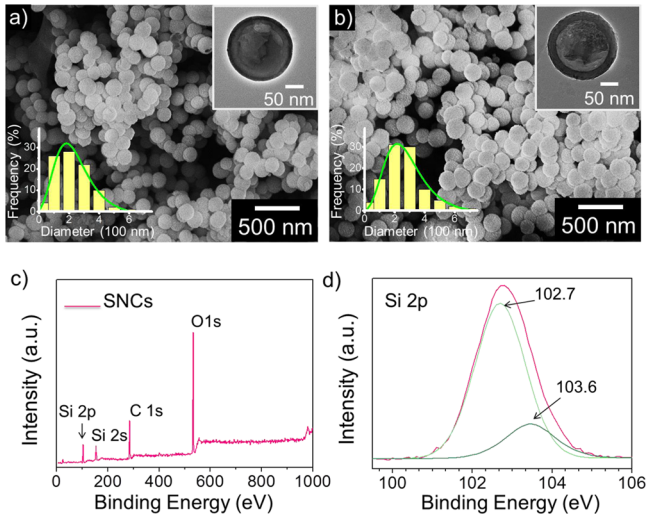

Figure 2. SEM images of SNCs: average core diameter (ca. 200 nm) with controlled shell thicknesses of (a) ca. 12 and (b) ca. 23 nm. The insets in a and b indicate TEM images and size-distribution diagrams of SNCs. (c) XPS spectra and (d) XPS Si 2p spectra of SNCs.

spherical with a well-defined hollow interior and dense shell of uniform thickness. Note that two different samples were prepared by adjusting the APES/TEOS molar ratios, one with a shell approximately 12 nm thick and the other with a shell approximately 23 nm thick. The core of the SNCs was approximately 200 nm in average diameter, but the diameter of these relatively polydisperse nanocapsules ranged from 100 to 400 nm (Figure 2a and b, insets), presumably due to uneven Ostwald ripening during the microemulsion procedure.[38] X-ray photoelectron spectroscopy (XPS; Sigma Probe) spectra of the SNCs showed Si 2p, Si 2s, and O 1s peaks (Figure 2c and SI Figure S2), with no evidence of impurities such as Pd and N atoms, suggesting that chromophores reside only within the capsules. Spectral deconvolution of the Si 2p peak (Figure 2d) suggested two peaks centered at 102.7 and 103.6 eV, consistent with the XPS spectrum of commercial SiO_2.[39,40] The C 1s peak is thought to have resulted from carbon tape (an adhesive).

The PdTPBP/perylene SNCs dispersed in water emitted intense upconverted blue light when irradiated with a 635 nm red laser (Figure 3a). It is noteworthy that efficient UC occurred in the aqueous phase even without deoxygenation. When stearic acid, a saturated fatty acid, was used as the core solvent instead of OA, similarly structured nanocapsules were obtained but did not produce any measurable UC emission (Figure 3b). This result confirms that the double bond in OA is necessary to quench the oxygen that otherwise prohibits TTET from triplet PdTPBP to perylene. The UC emission was also

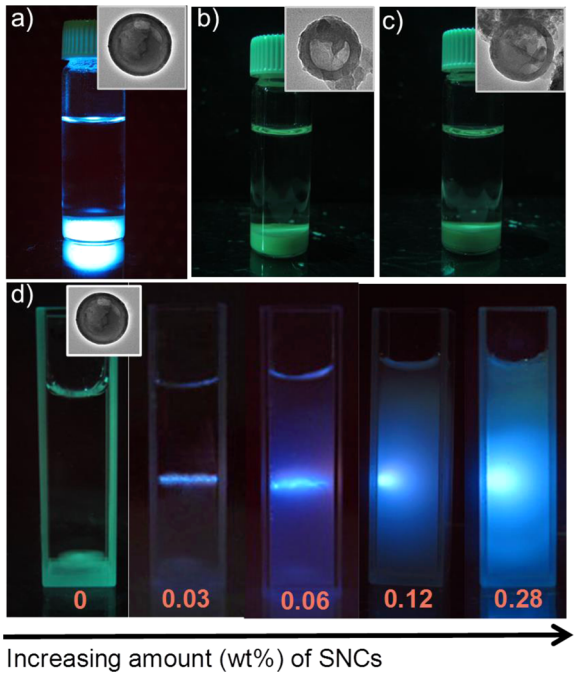

Figure 3. (a) Photograph of red-to-blue TTA-UC emission of OA-core SNCs (6 wt %) in water. (b, c) Photographs of stearic acid-core SNCs. (d) Photographs of TTA-UC emission from aqueous suspensions containing various concentrations of SNCs. A commercial diode 635 nm laser was used as the excitation source, and images were obtained using a 600 nm short-pass filter. The insets show TEM images of individual SNCs.

not observed when chromophores were embedded within the silica shell of SNCs with a stearic acid core (Figure 3c). This result confirms that UC in these SNCs originates from chromophores dissolved in the core phase, in contrast to other studies in which chromophores were embedded in porous solid particles.[28,30] The SNCs settle in a quiescent condition, but the suspension can be easily rehomogenized under gentle mixing. Upon irradiation with the red laser, UC emission was observed along the laser pathway in a suspension with a low nanocapsule concentration (0.03 wt %), but this emitted light diffused significantly in more concentrated SNC suspensions (Figure 3d). With SNCs at 0.28 wt %, diffused UC emission spanned the entire cuvette due to significant light diffraction by the nanocapsules. This is in stark contrast to UC in transparent organic solvent, where the UC occurs only through the laser pathway (Figure 1c, inset).

Figure 4 shows the emission spectra of TTA-UC SNCs dispersed in water upon laser excitation at 635 nm Both Stokes emission from ^{3}PdTPBP* phosphorescence at 750−850 nm and anti-Stokes upconverted emission from ^{1}perylene* fluorescence at 450−550 nm were evident and increased with increasing irradiation power. Note that the SNCs with the thinner shell (Figure 4a, 12 nm shell) emitted approximately twice as much upconverted light as those with the thicker shell (Figure 4b, 23 nm shell), presumably due to their less significant light obstruction[4,41] and to the greater number of the thin-shell SNCs preset per unit mass.[42] A thinner shell is therefore preferable, but SNCs with shells thinner than 10 nm were found to collapse when dried (SI Figure S3). The UC emission from both species of SNC increased with increasing irradiation power density (Figure 4c), exhibiting a quadratic power density dependence typical of TTA-UC in the weak-

DOI: 10.1021/am506233h
ACS Appl. Mater. Interfaces 2015, 7, 318−325

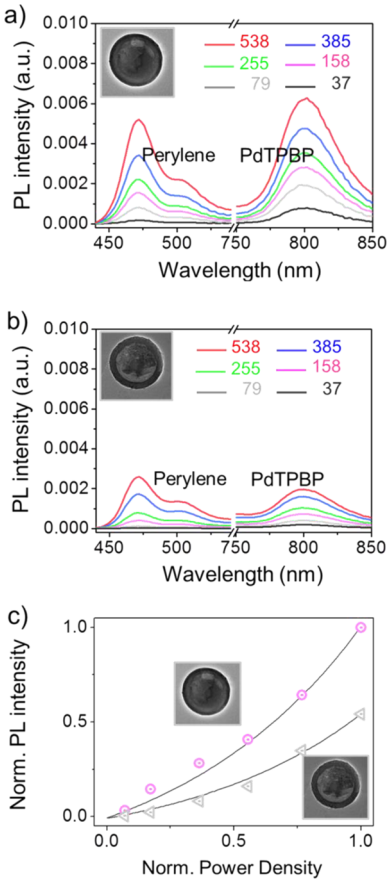

Figure 4. (a, b) Emission profiles of SNCs as a function of incident light power density (mW/cm^2) under excitation at 635 nm, where the SNCs have shells of thickness (a) ca. 12 nm and (b) ca. 23 nm. (c) Normalized integrated emission intensity as a function of normalized incident light power density for SNCs with shells of thickness ca. 12 nm (magenta) and ca. 23 nm (gray). The highest incident light power density was 538 mW/cm^2. Insets: TEM images of respective SNCs.

annihilation regime.[43] Pseudolinear or linear power dependence has been also reported using solvent as a host for TTA-UC chromophores but only at high laser power density,[21,22,28,43] which was difficult to achieve with the nanocapsule suspension due to significant light scattering.

The TTA-UC SNCs were further modified to demonstrate sub-bandgap photocatalysis in the aqueous phase. CdS nanoparticles (NPs) were directly deposited onto the surface of the silica shell to ensure close proximity of the site of UC emission to the site of photocatalysis. Direct surface loading has not been possible with either previously reported organic hosts for chromophore embedding[28,30] or capsules made of polymeric shells.[21,22,29] The nanocapsule surface was first functionalized with a silane coupling agent containing amino terminal groups ((3-aminopropyl)-trimethoxysilane) (APMS) (Step 1 in Figure 5).[40] The XPS spectrum of APMS-treated SNCs (Figure 6a) indicates the presence of N in addition to Si,

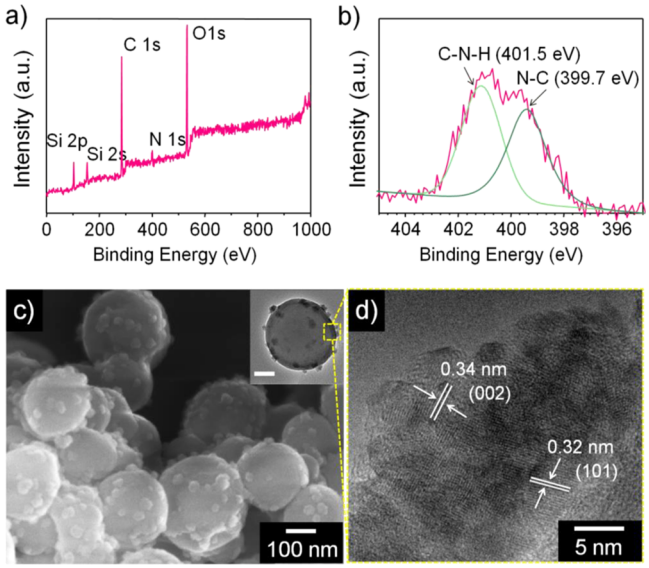

Figure 6. (a) Full XPS spectrum and (b) high-resolution XPS N 1s spectra of amine group functionalized-SNCs. (c) SEM and (d) HR-TEM images of CdS NPs-loaded SNCs (the scale bar in inset c is 50 nm).

C, and O without any impurities. Furthermore, the high-resolution XPS N 1s spectrum shows C−N−H and N−C peaks at 401.5 and 399.7 eV, respectively (Figure 6b), confirming successful amino-functionalization. The treated silica surface was then loaded with CdS NPs following the procedure outlined in Figure 5 (Step 2).[44] The color of the suspension changed from light green (amino-functionalized SNCs) to light yellow, indicating formation of CdS NP-loaded SNCs (CdS NPs/SNCs) (the insets in Figure 5). TEM analysis of the surface of the CdS NP-loaded SNCs as compared to the pristine SNC surface (Figure 2a and b) provides evidence of loading of the CdS NPs with diameters ranging from 6 to 20 nm (Figure 6c). These CdS NPs appeared to be polycrystalline

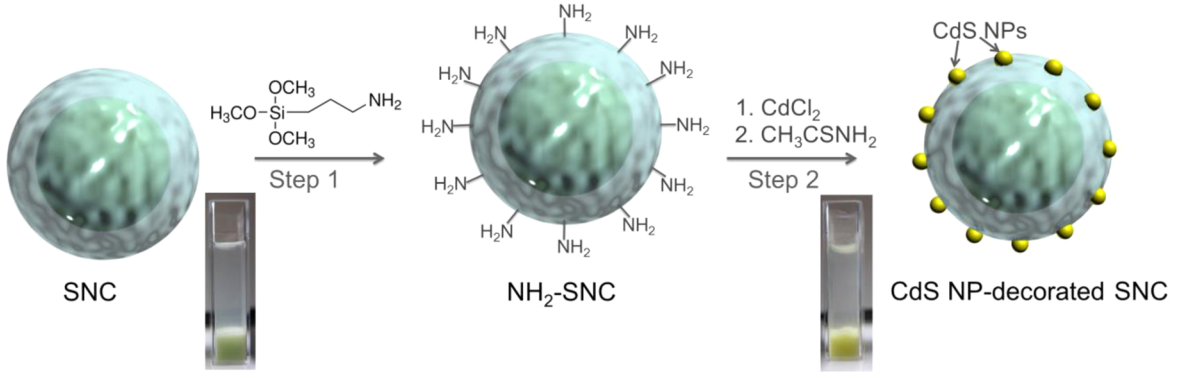

Figure 5. Fabrication procedure for CdS NP-loaded SNC via surface functionalization.

DOI: 10.1021/am506233h
ACS Appl. Mater. Interfaces 2015, 7, 318−325

with randomly arranged crystal lattices of consistent sizes, measured from the distance between crystal fringes in HR-TEM image (Figure 6d).[45,46]

To confirm sub-bandgap photocatalysis of CdS NP-decorated SNCs, we evaluated the generation of hydroxyl radical (•OH) under red laser excitation. The TTA-UC SNCs loaded with CdS NPs were dispersed in water containing coumarin, which reacts with hydroxyl radical (•OH) to form 7-hydroxycoumarin (Figure 7a).[45,47−49] Without TTA-UC,

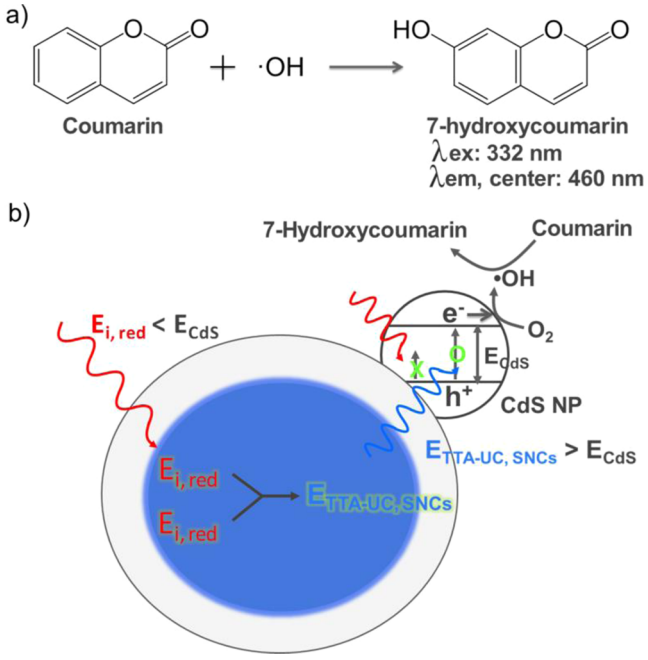

Figure 7. (a) Production of the coumarin−OH adduct (7-hydroxycoumarin) by the reaction of the coumarin (fluorescence probe) and •OH. (b) Schematic illustration of the mechanism of the sub-bandgap photocatalysis of the CdS-decorated SiO_2 nanocapsule TTA-UC system.

irradiation with 635 nm (1.95 eV) light would not activate CdS NPs (E_g = 2.4 eV) and •OH would therefore not be generated (Figure 7b). With the CdS NP-loaded TTA-UC nanocapsules, the upconverted emission resulting from 635 nm irradiation is reabsorbed by the CdS NPs (SI Figure S4), leading to CdS sensitization. The resulting formation of •OH was confirmed by the increase of 7-hydroxycoumrain fluorescence emission at 460 nm (Figure 8). Note that •OH forms in this case via formation of the superoxide radical anion as an intermediate ($O_2/O_2^{\bullet-}$: −0.28 eV) through the transfer of one electron from the CdS conduction band.[50−52] When the CdS NP-decorated SNCs contained only PdTPBP or only perylene, negligible 7-hydroxycoumrain formation was observed, confirming that the CdS NPs could be sensitized only when incident light was upconverted. Accordingly, the •OH production was dependent on the incident light power density and the reaction time. This result is the first example of the production of •OH by photons in the red region via photon frequency amplification.

CONCLUSION

The TTA-UC architecture presented herein is unprecedented in the literature in its nanoscale dimension, structural rigidity, and surface functionalizability; the combination of which

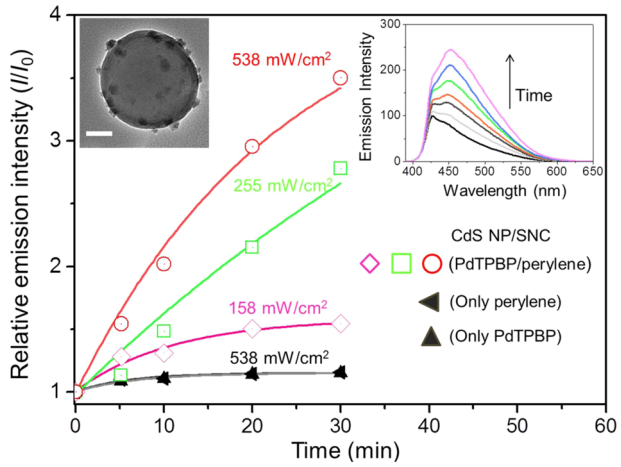

Figure 8. Examination of the formation of •OH through monitoring of emission intensity of the coumarin−OH adduct at 460 nm. CdS NP-decorated SNC contained PdTPBP and perylene, only perylene, or only PdTPBP. Insets: time-dependent fluorescence spectra (538 mW/cm²), TEM image of the CdS NP-decorated SNCs used in this system.

should facilitate various aqueous-phase applications. Through the incorporation of further functionalities, it is expected that a wide range of aqueous-based applications can be developed, including visible light-driven photocatalysis, demonstrated herein, for the first time, to produce •OH via frequency amplification of 635 nm red light. Potential applications include not only aqueous photocatalysis (e.g., environmental remediation) but also TTA-UC-enhanced artificial photosynthesis and bioimaging (e.g., two photon microscopy).

ASSOCIATED CONTENT

Supporting Information

Additional information about the TTA-UC mechanism, quantum yield measurement, sample characterization with XPS and SEM, and changes in emission spectra due to CdS NP loading onto the SNCs. This material is available free of charge via the Internet at http://pubs.acs.org.

AUTHOR INFORMATION

Corresponding Author

*E-mail: jaehong.kim@yale.edu. Tel: +1-203-432-4386. Fax: +1-203-432-4387.

Notes

The authors declare no competing financial interest.

ACKNOWLEDGMENTS

This work was supported by the National Science Foundation (CBET-1033866).

REFERENCES

(1) Martín-Rodríguez, R.; Fischer, S.; Ivaturi, A.; Froehlich, B.; Krämer, K. W.; Goldschmidt, J. C.; Richards, B. S.; Meijerink, A. Highly Efficient IR to NIR Upconversion in $Gd_2O_2S:Er^{3+}$ for Photovoltaic Applications. *Chem. Mater.* **2013**, *25*, 1912−1921.

(2) Wang, H.-Q.; Batentschuk, M.; Osvet, A.; Pinna, L.; Brabec, C. J. Rare-Earth Ion Doped Upconversion Materials for Photovoltaic Applications. *Adv. Mater.* **2011**, *23*, 2675−2680.

(3) Shpaisman, H.; Niitsoo, O.; Lubomirsky, I.; Cahen, D. Can Up- and Down-Conversion and Multi-Exciton Generation Improve Photovoltaics? *Sol. Energy Mater. Sol. Cells* **2008**, *92*, 1541−1546.

DOI: 10.1021/am506233h
ACS Appl. Mater. Interfaces 2015, 7, 318−325

(4) Du, Y.; Luna, L. E.; Tan, W. S.; Rubner, M. F.; Cohen, R. E. Hollow Silica Nanoparticles in UV−Visible Antireflection Coatings for Poly(methyl methacrylate) Substrates. *ACS Nano* **2010**, *4*, 4308−4316.
(5) Jankus, V.; Snedden, E. W.; Bright, D. W.; Whittle, V. L.; Williams, J. A. G.; Andy Monkman, A. Energy Upconversion via Triplet Fusion in Super Yellow PPV Films Doped with Palladium Tetraphenyltetrabenzoporphyrin: A Comprehensive Investigation of Exciton Dynamics. *Adv. Funct. Mater.* **2013**, *23*, 384−393.
(6) Li, C.; Yang, X.; Jimmy, C. Y.; Ming, T.; Wang, J. Porous Upconversion Materials-Assisted Near Infrared Energy Harvesting by Chlorophylls. *Chem. Commun.* **2011**, *47*, 3511−3513.
(7) Wang, Y.-L.; Nan, F.; Liu, X.-L.; Zhou, L.; Peng, X.-N.; Zhou, Z.-K.; Yu, Y.; Hao, Z.-H.; Wu, Y.; Zhang, W. Plasmon-Enhanced Light Harvesting of Chlorophylls on Near-Percolating Silver Films via One-Photon Anti-Stokes Upconversion. *Sci. Rep.* **2013**, *3*, 1−7.
(8) Islangulov, R. R.; Castellano, F. N. Photochemical Upconversion: Anthracene Dimerization Sensitized to Visible Light by a Ru II Chromophore. *Angew. Chem.* **2006**, *118*, 6103−6105.
(9) Li, H.; He, X.; Kang, Z.; Huang, H.; Liu, Y.; Liu, J.; Lian, S.; Tsang, C. H. A.; Yang, X.; Lee, S.-T. Water-Soluble Fluorescent Carbon Quantum Dots and Photocatalyst Design. *Angew. Chem., Int. Ed.* **2010**, *49*, 4430−4434.
(10) Zhuo, S.; Shao, M.; Lee, S.-T. Upconversion and Down-conversion Fluorescent Graphene Quantum Dots: Ultrasonic Preparation and Photocatalysis. *ACS Nano* **2012**, *6*, 1059−1064.
(11) Tian, J.; Sang, Y.; Yu, G.; Jiang, H.; Mu, X.; Liu, H. A Bi_2WO_6-Based Hybrid Photocatalyst with Broad Spectrum Photocatalytic Properties under UV, Visible, and Near-Infrared Irradiation. *Adv. Mater.* **2013**, *25*, 5075−5080.
(12) Ji, S.; Guo, H.; Wu, W.; Wu, W.; Zhao, J. Ruthenium(II) Polyimine−Coumarin Dyad with Non-emissive ^{3}IL Excited State as Sensitizer for Triplet−Triplet Annihilation Based Upconversion. *Angew. Chem., Int. Ed.* **2011**, *50*, 8283−8286.
(13) Shao, M.; Zhuo, S. Reply to "Comment on 'Upconversion and Downconversion Fluorescent Graphene Quantum Dots: Ultrasonic Preparation and Photocatalysis'. *ACS Nano* **2012**, *6*, 6532−6532.
(14) Kumar, R.; Nyk, M.; Ohulchanskyy, T. Y.; Flask, C. A.; Prasad, P. N. Combined Optical and MR Bioimaging Using Rare Earth Ion Doped $NaYF_4$ Nanocrystals. *Adv. Funct. Mater.* **2009**, *19*, 853−859.
(15) Li, Z.; Zhang, Y.; Jiang, S. Multicolor Core/Shell-Structured Upconversion Fluorescent Nanoparticles. *Adv. Mater.* **2008**, *20*, 4765−4769.
(16) Zhang, F.; Che, R.; Li, X.; Yao, C.; Yang, J.; Shen, D.; Hu, P.; Li, W.; Zhao, D. Direct Imaging the Upconversion Nanocrystal Core/Shell Structure at the Subnanometer Level: Shell Thickness Dependence in Upconverting Optical Properties. *Nano Lett.* **2012**, *12*, 2852−2858.
(17) Zhao, J.; Jin, D.; Schartner, E. P.; Lu, Y.; Liu, Y.; Zvyagin, A. V.; Zhang, L.; Dawes, J. M.; Xi, P.; Piper, J. A. Single-Nanocrystal Sensitivity Achieved by Enhanced Upconversion Luminescence. *Nat. Nanotechnol.* **2013**, *8*, 729−734.
(18) Zhang, C.; Lee, J. Y. Prevalence of Anisotropic Shell Growth in Rare Earth Core−Shell Upconversion Nanocrystals. *ACS Nano* **2013**, *7*, 4393−4402.
(19) Ni, D.; Zhang, J.; Bu, W.; Xing, H.; Han, F.; Xiao, Q.; Yao, Z.; Chen, F.; He, Q.; Liu, J.; Zhang, S.; Fan, W.; Zhou, L.; Peng, W.; Shi, J. Dual-Targeting Upconversion Nanoprobes across the Blood−Brain Barrier for Magnetic Resonance/Fluorescence Imaging of Intracranial Glioblastoma. *ACS Nano* **2014**, *8*, 1231−1242.
(20) Zhao, J.; Ji, S.; Guo, H. Triplet−Triplet Annihilation based Upconversion: From Triplet Sensitizers and Triplet Acceptors to Upconversion Quantum Yields. *Rsc Adv.* **2011**, *1*, 937−950.
(21) Kim, J.-H.; Kim, J.-H. Encapsulated Triplet−Triplet Annihilation-based Upconversion in the Aqueous Phase for Sub-Band-Gap Semiconductor Photocatalysis. *J. Am. Chem. Soc.* **2012**, *134*, 17478−17481.
(22) Liu, Q.; Yin, B.; Yang, T.; Yang, Y.; Shen, Z.; Yao, P.; Li, F. A General Strategy for Biocompatible, High-Effective Upconversion Nanocapsules based on Triplet−Triplet Annihilation. *J. Am. Chem. Soc.* **2013**, *135*, 5029−5037.
(23) Singh-Rachford, T. N.; Castellano, F. N. Supra-Nanosecond Dynamics of a Red-to-Blue Photon Upconversion System. *Inorg. Chem.* **2009**, *48*, 2541−2548.
(24) Svagan, A.; Busko, D.; Avlaseich, Y.; Glasser, G.; Baluschev, S.; Landfester, K. Photon Energy Upconversion Nanopaper: A Bio-inspired Oxygen Protection Strategy. *ACS Nano* **2013**, *8*, 8198−8207.
(25) Zhang, N.; Liu, S.; Xu, Y.-J. Recent Progress on Metal Core@ Semiconductor Shell Nanocomposites as a Promising Type of Photocatalyst. *Nanoscale* **2012**, *4*, 2227−2238.
(26) Zhou, H.; Qu, Y.; Zeid, T.; Duan, X. Towards Highly Efficient Photocatalysts using Semiconductor Nanoarchitectures. *Energy Environ. Sci.* **2012**, *5*, 6732−6743.
(27) Kisch, H. Semiconductor Photocatalysis—Mechanistic and Synthetic Aspects. *Angew. Chem., Int. Ed.* **2013**, *52*, 812−847.
(28) Monguzzi, A.; Frigoli, M.; Larpent, C.; Tubino, R.; Meinardi, F. Low-Power-Photon Upconversion in Dual-Dye-Loaded Polymer Nanoparticles. *Adv. Funct. Mater.* **2012**, *22*, 139−143.
(29) Wohnhaas, C.; Turshatov, A.; Mailänder, V.; Lorenz, S.; Baluschev, S.; Miteva, T.; Landfester, K. Annihilation Upconversion in Cells by Embedding the Dye System in Polymeric Nanocapsules. *Macromol. Biosci.* **2011**, *11*, 772−778.
(30) Liu, Q.; Yang, T.; Feng, W.; Li, F. Blue-Emissive Upconversion Nanoparticles for Low-Power-Excited Bioimaging In Vivo. *J. Am. Chem. Soc.* **2012**, *134*, 5390−5397.
(31) Andrey, T.; Dmitry, B.; Stanislav, B.; Tzenka, M.; Katharina, L. Micellar Carrier for Triplet−Triplet Annihilation-Assisted Photon Energy Upconversion in a Water Environment. *New J. Phys.* **2011**, *13*, 083035.
(32) YaoáZheng, J.; ShengáZhao, Y. Electrogenerated Upconverted Emission from Doped Organic Nanowires. *Chem. Commun.* **2012**, *48*, 85−87.
(33) Tanaka, K.; Okada, H.; Ohashi, W.; Jeon, J.-H.; Inafuku, K.; Chujo, Y. Hypoxic Condition-Selective Upconversion via Triplet−Triplet Annihilation based on POSS−Core Dendrimer Complexes. *Bioorg. Med. Chem.* **2013**, *21*, 2678−2681.
(34) Tanaka, K.; Inafuku, K.; Chujo, Y. Environment-Responsive Upconversion based on Dendrimer-Supported Efficient Triplet−Triplet Annihilation in Aqueous Media. *Chem. Commun.* **2010**, *46*, 4378−4380.
(35) Askes, S. H.; Bahreman, A.; Bonnet, S. Activation of a Photodissociative Ruthenium Complex by Triplet−Triplet Annihilation Upconversion in Liposomes. *Angew. Chem.* **2014**, *126*, 1047−1051.
(36) Han, L.; Gao, C.; Wu, X.; Chen, Q.; Shu, P.; Ding, Z.; Che, S. Anionic Surfactants Templating Route for Synthesizing Silica Hollow Spheres with Different Shell Porosity. *Solid State Sci.* **2011**, *13*, 721−728.
(37) Kim, J.-H.; Deng, F.; Castellano, F. N.; Kim, J.-H. Red-to-Blue/Cyan/Green Upconverting Microcapsules for Aqueous-and Dry-Phase Color Tuning and Magnetic Sorting. *ACS Photonics* **2014**, *1*, 382−388.
(38) Cushing, B. L.; Kolesnichenko, V. L.; O'Connor, C. J. Recent Advances in the Liquid-Phase Syntheses of Inorganic Nanoparticles. *Chem. Rev.* **2004**, *104*, 3893−3946.
(39) Feng, L.; Li, H.; Yang, M.; Wang, X. Synthesis of SiO_2/Polystyrene Hybrid Particles via an Esterification Method. *Colloid Polym. Sci.* **2010**, *288*, 673−680.
(40) Kwon, O. S.; Ahn, S. R.; Park, S. J.; Song, H. S.; Lee, S. H.; Lee, J. S.; Hong, J.-Y.; Lee, J. S.; You, S. A.; Yoon, H. Ultrasensitive and Selective Recognition of Peptide Hormone Using Close-Packed Arrays of hPTHR-Conjugated Polymer Nanoparticles. *ACS Nano* **2012**, *6*, 5549−5558.
(41) Gao, T.; Jelle, B. P.; Gustavsen, A. Antireflection Properties of Monodisperse Hollow Silica Nanospheres. *Appl. Phys. A: Mater. Sci. Process.* **2013**, *110*, 65−70.
(42) Oh, W.-K.; Kwon, O. S.; Jang, J. Conducting Polymer Nanomaterials for Biomedical Applications: Cellular Interfacing and Biosensing. *Polym. Rev.* **2013**, *53*, 407−442.

DOI: 10.1021/am506233h
ACS Appl. Mater. Interfaces 2015, 7, 318−325

(43) Singh-Rachford, T. N.; Castellano, F. N. Photon Upconversion based on Sensitized Triplet−Triplet Annihilation. *Coord. Chem. Rev.* **2010**, *254*, 2560−2573.
(44) Fan, D.; Afzaal, M.; Mallik, M. A.; Nguyen, C. Q.; O'Brien, P.; Thomas, P. J. Using Coordination Chemistry to Develop New Routes to Semiconductor and Other Materials. *Coord. Chem. Rev.* **2007**, *251*, 1878−1888.
(45) Lin, G.; Zheng, J.; Xu, R. Template-Free Synthesis of Uniform CdS Hollow Nanospheres and Their Photocatalytic Activities. *J. Phys. Chem. C* **2008**, *112*, 7363−7370.
(46) Lippens, P.; Lannoo, M. Calculation of the Band Gap for Small CdS and ZnS Crystallites. *Phys. Rev. B* **1989**, *39*, 10935−10942.
(47) Li, X.; Gao, Y.; Yu, L.; Zheng, L. Template-Free Synthesis of CdS Hollow Nanospheres based on an Ionic Liquid Assisted Hydrothermal Process and Their Application in Photocatalysis. *J. Solid State Chem.* **2010**, *183*, 1423−1432.
(48) Tang, W. Z.; Huang, C. Photocatalyzed Oxidation Pathways of 2,4-dichlorophenol by CdS in Basic and Acidic Aqueous Solutions. *Water Res.* **1995**, *29*, 745−756.
(49) Huang, Y.; Sun, F.; Wu, T.; Wu, Q.; Huang, Z.; Su, H.; Zhang, Z. Photochemical Preparation of CdS Hollow Microspheres at Room Temperature and Their Use in Visible-Light Photocatalysis. *J. Solid State Chem.* **2011**, *184*, 644−648.
(50) Huang, S.; Lin, Y.; Yang, J.; Li, X.; Zhang, J.; Yu, J.; Shi, H.; Wang, W.; Yu, Y. Enhanced Photocatalytic Activity and Stability of Semiconductor by Ag Doping and Simultaneous Deposition: The Case of CdS. *Rsc Adv.* **2013**, *3*, 20782−20792.
(51) Luo, M.; Liu, Y.; Hu, J.; Liu, H.; Li, J. One-Pot Synthesis of CdS and Ni-Doped CdS Hollow Spheres with Enhanced Photocatalytic Activity and Durability. *ACS Appl. Mater. Interfaces* **2012**, *4*, 1813−1821.
(52) Zhang, X.; Chen, Y. L.; Liu, R.-S.; Tsai, D. P. Plasmonic Photocatalysis. *Rep. Prog. Phys.* **2013**, *76*, 046401.

DOI: 10.1021/am506233h
ACS Appl. Mater. Interfaces 2015, 7, 318−325